Demonstration of First-Principle Data-Driven models using numerical case studies

P. Czop [a,*], D. Sławik [a], G. Wszołek [b]

[a] Tenneco Automotive Eastern Europe, Eastern European Engineering Center (EEEC), ul. Bojkowska 59 B, 44-100 Gliwice, Poland

[b] Institute of Engineering Processes Automation and Integrated Manufacturing Systems, Silesian University of Technology, ul. Konarskiego 18a, 44-100 Gliwice, Poland

* Corresponding author: E-mail address: piotr.czop@labmod.com

Analysis and modelling

ABSTRACT

Purpose: The paper consists of two parts. The first part presents and discusses a process of formulation and identification of First-Principle Data-Driven (FPDD) models, while the second part demonstrates numerical examples of identification of FPDD models.

Design/methodology/approach: First-Principle (FP) model is formulated using a system of continuous ordinary differential equations capturing usually nonlinear relations among variables of the model. The considering model applies three categories of parameters: geometrical, physical and phenomenological. Geometrical and physical parameters are deduced from construction or operational documentation. The phenomenological parameters are the adjustable ones, which are estimated or adjusted based on their roughly known values, e.g. friction/damping coefficients.

Findings: A few phenomenological parameters were successfully estimated from numerically generated data. The error between the true and estimated value of the parameter occurred, however its magnitude is low at level below 2%.

Research limitations/implications: Adjusting a model to data is, in most cases, a non-convex optimization problem and the criterion function may have several local minima. This is a case when multiple parameters are simultaneously estimated.

Practical implications: FPDD models are an excellent tool for understanding, optimizing, designing, and diagnosing technical systems since they are updatable using operational measurements. This opens application area, for example, for model-based design and early warning diagnostics.

Originality/value: First-Principle (FP) models are frequently adjusted by trial-and-error, which can lead to non-optimal results. In order to avoid deficiencies of the trial-and-error approach, a formalized mathematical method using optimization techniques to minimize the error criterion, and find optimal values of tunable model parameters, was proposed and demonstrated in this work.

Keywords: First-Principle model, Data Driven model, Grey-box, Servo-hydraulic system

1. Basic demonstration

This section presents an example of parameter adjustment of FP (First-Principle) model based on a simulated data from a continuous-time state-space model. This model may refer to mechanical second order system, i.e. harmonic resonator with linear damping. The input *u(t)* to the system is the force and the measured output *y(t)* is the displacement. The system is described by the following differential equation

$$m\frac{d^2x}{dt^2} + d\frac{dx}{dt} + kx = u, \quad y = x \tag{1}$$

This equation can be transferred into state-space representation

$$\dot{x} = Ax + Bu$$
$$y = Cx + Du \tag{2}$$

where particular matrices A, B, C, and D are as follows

$$A = \begin{bmatrix} 0 & 1 \\ -k/m & -d/m \end{bmatrix}, \ B = \begin{bmatrix} 0 \\ 1/m \end{bmatrix},$$
$$C = \begin{bmatrix} 1 & 0 \end{bmatrix}, \text{D=0} \tag{3}$$
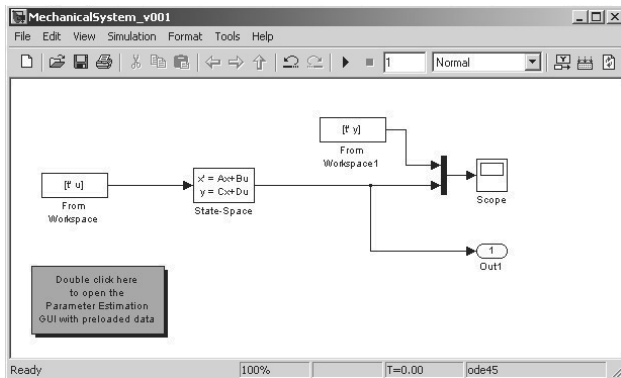
Fig. 1. A system model implemented in Simulink as the state space equations

The model was implemented in Simulink and run to generate input-output data sets which are used in Sections 1.1 and 1.2.

1.1. Estimation with use of System Identification Toolbox

System Identification Toolbox is designed to work in Matlab environment. It provides a library of system identification routines for black-box and grey-box models.

In the case A, *m* and *k* parameters are the fix parameters (known a priori), while parameter *d* is the free parameter (unknown) estimating from available input-output data (Table 1).

The error is calculated between the value of the system parameters and the estimated free parameters

Table 1.
Free and known system parameters (case A)

Parameter	m	d	k
System parameters	1	0.1	3947.8
Free parameters (unknown)		d	k
Fix parameters (known)	m		
Estimated free parameters		0.099987	3949.9
Error		0.0013%	0.0532%

In the case B, *m* parameter is the fix parameter, while parameters *d* and *k* are the free parameters estimating from available input-output data (Table 2). The error is calculated between the value of the system parameters, and the estimated free parameter.

Table 2.
Free and known system parameters (case B)

Parameter	m	d	k
System parameters	1	0.1	3947.8
Free parameters (unknown)		d	
Fix parameters (known)	m		k
Estimated free parameters		0.10323	
Error		2%	

1.2. Estimation with use of Simulink® Parameter Estimation tool

Simulink® Parameter Estimation™ uses optimization techniques to estimates the values of parameters and (optionally) initial conditions of states such that a user-selected cost function is minimized. The cost function typically calculates a least-squares error between the empirical and model input-output data. The Control and Estimation Tools Manager, which is a graphical user interface (GUI) for performing parameter estimation, stores and organizes all data from a given Simulink model inside a project (Fig. 3a). A system identification project was created using Control and Estimation Tool Manager (Fig. 2).

In the case C, as the free parameters were selected damping *d*, and stiffness *k*, while mass *m* was defined as the fix parameter (Table 3). In the case D, as the free parameter was selected stiffness *k*, while mass *m* and damping *d* were defined as the fix parameters (Table 4). The boundary conditions were imposed on the estimating parameters values (Fig. 2).

Fig. 2. Control and Estimation Tools Manager

The trend of parameters variability during convergence (optimization) process was shown in Fig. 4. The comparison of the proposed system identification tools is in Table 7.

The criterion "Simulink support" in the Table 7 enables system identification using the equations directly implemented in Simulink. The criterion "Convergence performance" evaluates time consumed by the simulation, while 'convergence robustness" evaluates possibility to get incorrect results, e.g. no solution, local minimum.

Table 3.
Free and known system parameters (case C)

Parameter	m	d	k
System parameters	1	0.1	3947.8
Free parameters (unknown)		d	k
Fix parameters (known)	m		
Estimated free parameters		0.099987	3947.8
Error		0.0014%	0%

The iterative convergence process was run for a couple of seconds (below 1 min) to optimize the error objective function. Simulation and optimization settings used the parameter adjustment process are presented in Table 5+6. The Newton-Gauss method, lsqnonlin(.) routine implemented in the Optimization Toolbox of Matlab, was used to minimize the function describing the error in the model outputs.

Table 4.
Free and known system parameters (case D)

Parameter	m	d	k
System parameters	1	0.1	3947.8
Free parameters (unknown)		d	
Fix parameters (known)	m		k
Estimated free parameters		0.099987	
Error		0.0013%	

The error was computed comparing reference system output (displacement) with predicted model output after each iteration.

Table 5.
Simulation settings

Option	Value
Solver	ode23tb (stiff/TR-BDF2)
Max step size	auto
Min step size	auto
Zero crossing control	disable all
Relative tolerance	auto
Absolute tolerance	auto

Table 6.
Optimization (minimization) settings

Option	Value
Gradient type	basic
Algorithm	lsqnonlin
Cost type	SSE
DiffMaxChange	0.1
DiffMinChange	1E-08
Large scale	true
MaxIter	28
RobustCost	False
TolCon	1E-6
TolFun	1E-6

Table 7.
Comparison of grey-box system identification tools

Tool / Property	System Identification Toolbox	Simulink® Parameter Estimation™
On-line identification	yes	no
Simulink support	no	yes
Nonlinear models support	yes	yes
Convergence performance	moderate	low
Convergence robustness	good	low
Multiple output model support	no	yes

A process of model adjustment is visualized in Fig. 3 after a specific number of iterations.

a)

b)

c)
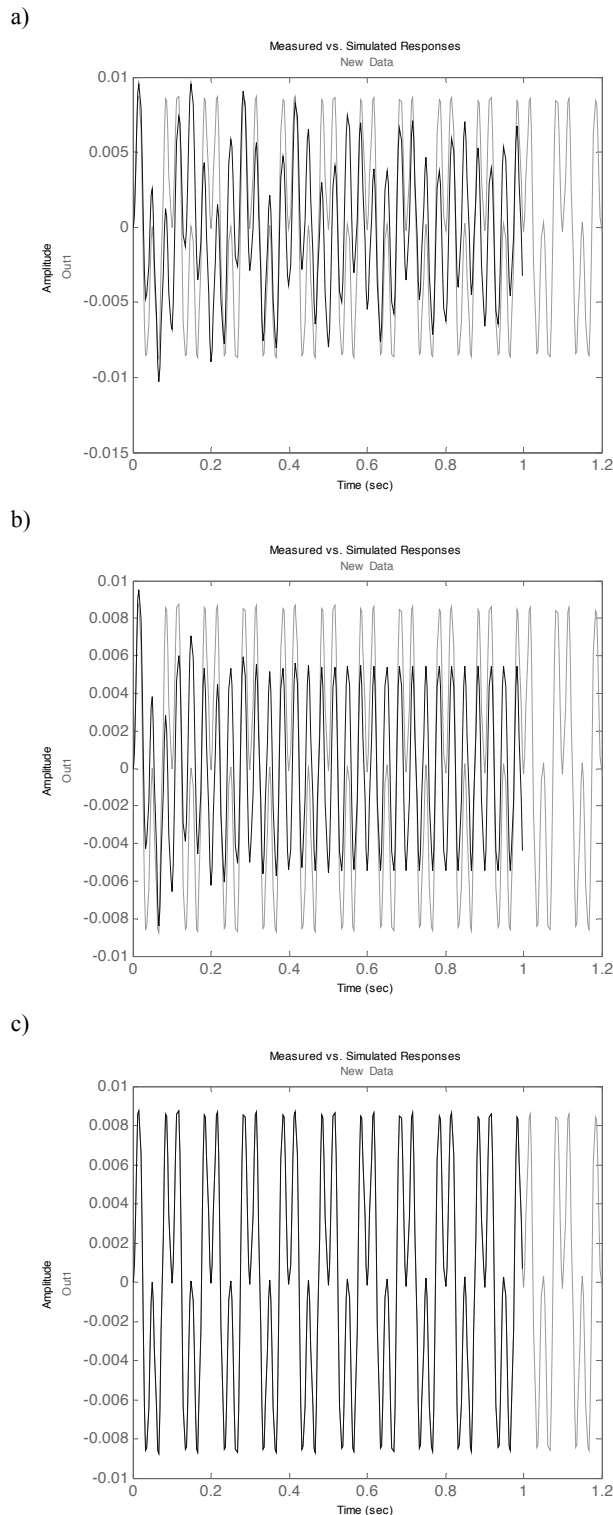
Fig. 3. Convergence progress (reference model response - grey, optimized model response - dark grey): a) 3rd iteration, b) 10th iteration, c) 20th iteration
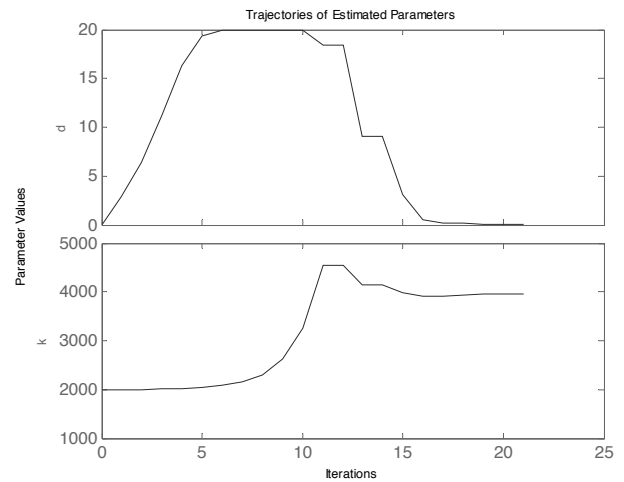
Fig. 4. Trends of the estimating parameters

2. Advanced demonstration

This advanced example demonstrates estimation of parameters of a continuous-time model based on the servo-hydraulic test rig. The model is developed for the Hydropuls® MSP25 servo-hydraulic test-rig, equipped with an IST8000 electronic controller. The test rig is equipped with an oil supply system (the so-called servo-pack) that provides a pressure of 28 MPa at a flow-rate of 90 l/min. The actuator provides a 25 kN force at the rod, while the maximum stroke is 250 mm at the maximum achievable velocity of 3 m/s. The main components of the servo-hydraulic system are the hydraulic actuator with integrated displacement transducer in a piston-rod assembly (IST-Schenk) and the three-stage servo-valve system. The test rig is equipped with a PID controller. The excitation signal is converted into a voltage applied to the servo-valve, which controls the amount of oil supplied to the chambers of the actuator.

2.1. Formulation of FP model

The simulation FP model of the Hydropuls® MSP25 test-rig consists of a servo-valve and a hydraulic actuator model. The Moog G761 series (Fig. 5) industrial servo-valve consists of a polarized electrical torque motor and two stages of hydraulic power amplification. This valve dynamics is approximated by a transfer function whose input is a voltage and output is the spool displacement.

The electromagnetic torque motor, driving the flapper, is controlled by an electrical current inputted from a current amplifier. A valve control input u (voltage) is converted into a current, with a current amplifier gain K_e. The hydrodynamic forces acting on the spool are neglected. Therefore, the spool position depends on the input voltage, angular natural frequency $\omega_{n,servo}$ and damping ratio of the servovalve ζ.
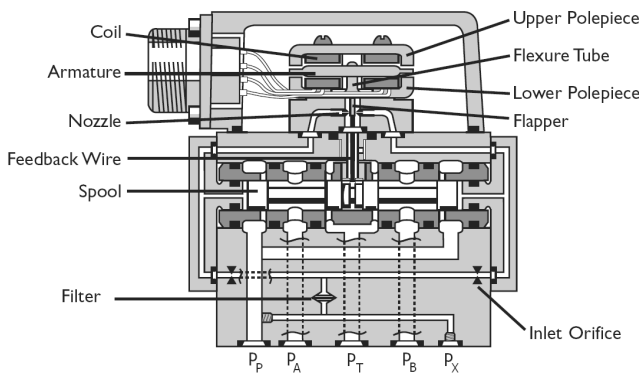
Fig. 5. The MOOG G761 servo-valve assembly

$$G_{servo} = \frac{x_{spool}(s)}{u_{PID}(s)} = \frac{K_e \cdot K_{spool}}{1 + \left(\dfrac{2\zeta}{\omega_{n,servo}}\right)s + \left(\dfrac{s}{\omega_{n,servo}}\right)^2} \qquad (4)$$

The pressure drops among the test rig chambers (A and B), input (P) and output (T) are as follows

$$\begin{aligned}
\Delta p_{PA} &= p_P - p_A \\
\Delta p_{BT} &= p_B - p_T \\
\Delta p_{AT} &= p_A - p_T \\
\Delta p_{PB} &= p_P - p_B
\end{aligned} \qquad (5)$$

The flows at all servovalve restrictions are determined by orifice equations based on pressure drops and spool displacement.

$$\begin{aligned}
q_{PA} &= Cd_{PA} \cdot b \cdot |\Delta x_{spool}| \cdot \sqrt{2|\Delta p_{PA}|/\rho} \cdot \mathrm{sgn}(\Delta p_{PA}) \\
&\text{if} \quad \Delta x_{spool} = x_{spool} - x_{spool,0} \geq 0 \\
q_{BT} &= Cd_{BT} \cdot b \cdot |\Delta x_{spool}| \cdot \sqrt{2|\Delta p_{BT}|/\rho} \cdot \mathrm{sgn}(\Delta p_{BT}) \\
&\text{if} \quad \Delta x_{spool} = x_{spool} - x_{spool,0} \geq 0 \\
q_{AT} &= Cd_{AT} \cdot b \cdot |\Delta x_{spool}| \cdot \sqrt{2|\Delta p_{AT}|/\rho} \cdot \mathrm{sgn}(\Delta p_{AT}) \\
&\text{if} \quad \Delta x_{spool} = x_{spool} + x_{spool,0} < 0 \\
q_{PB} &= Cd_{PB} \cdot b \cdot |\Delta x_{spool}| \cdot \sqrt{2|\Delta p_{PB}|/\rho} \cdot \mathrm{sgn}(\Delta p_{PB}) \\
&\text{if} \quad \Delta x_{spool} = x_{spool} + x_{spool,0} < 0
\end{aligned} \qquad (6)$$

In case of hydraulic machine we can assume density of oil as constant because for maximal load (pressure drop=150 bar) the hydraulic oil density change 1% that give 0.5% change in flow. For pressure drop 10 bar change in flow is smaller than 0.034%.

A model of a hydraulic actuator is derived assuming the pressures in the actuator chambers and displacement of the rod as the state variables. The bypass flow, controlled by the throttle valve, is defined by the following formula

$$q_{AB} = Cd_{AB} \cdot A_{leak} \cdot \sqrt{2|\Delta p_{AB}|/\rho} \cdot \mathrm{sgn}(\Delta p_{AB}) \qquad (7)$$

The total balance of the inlet and outlet flows is determined as follows

$$\begin{aligned}
q_A &= q_{PA} - q_{AT} - q_{AB} \\
q_B &= q_{PB} - q_{BT} + q_{AB}
\end{aligned} \qquad (8)$$

The pressures p_A and p_B are determined based on the mass equilibrium equations, where the volumes are determined based on the initial oil volume in the actuator and the position of the piston-rod

$$\begin{aligned}
\frac{dp_A}{dt} &= \frac{(q_A - \dot{V}_A) \cdot B}{V_{A0} + A_A \cdot x} \\
\frac{dp_B}{dt} &= \frac{(q_B + \dot{V}_B) \cdot B}{V_{B0} - A_B \cdot x}
\end{aligned} \qquad (9)$$

were changes of chamber volumes

$$\dot{V}_A = A_A \dot{x}, \ \dot{V}_B = A_B \dot{x} \qquad (10)$$

Finally, the displacement of the actuator x is calculated based on the force equilibrium equation

$$\ddot{x}m + F_{fric}(\dot{x}) = p_A A_A - p_B A_B - F_{ext}(x, \dot{x}) \qquad (11)$$

where: A_A, A_B are the pressure acting areas of two sides of the piston; p_A, p_B are the pressures in the chambers. The dry friction force F_{fric} between the piston and cylinder and rod and seal is modelled as follows:

$$F_{fric} = F_{fric\_max} \cdot \tanh\left(\frac{\dot{x}}{v_{ref}}\right) \qquad (12)$$

The friction force F_{fric} depends on the direction of the rod travel x, not on velocity nor piston position. The maximal friction force F_{fric_max} is obtained from experimental tests. The applied friction model uses the hyperbolic tangent function tanh(.) which approximates measurement data and the reference velocity v_{ref} which provides a smooth (realistic) switch of friction force similar to measurement data.

A model of the electronic controller uses a program command and sensor feedback to control the servovalve. A test rig controller uses a group of gain controls, i.e. proportional (P), integral (I) and derivative (D) gains. A transfer function representation of a PID controller is given as follows

$$\begin{aligned}
G_{PID} &= \frac{u_{PID}(s)}{\Delta x(s)} = K_P\left(1 + \frac{1}{sT_I} + sT_D\right) = \ldots \\
&= K_P + \frac{K_I}{s} + K_D s
\end{aligned} \qquad (13)$$

P. Czop, D. Sławik, G. Wszołek

where

$$\Delta x = x_{exp} - x. \tag{14}$$

The output u_{PID} of the PID controller is used as input of servovalve transfer function. The equations have been implemented in the MATLAB/Simulink package [1].

Table 8.
Values of fixed model parameters

Configuration parameters	Values
PID controls	
PID proportional gain K_P	400 [V/m]
PID integral gain K_I	0 [V·s/m]
PID derivative gain K_D	0 [V/(m·s)]
Hydraulic actuator	
oil density	960 [kg/m³]
chamber volume V_A and V_B	480 [ccm]
pressure acting area A_A and A_B	1920 [mm²]
Piston-rod assembly mass m	45 [kg]
fluid bulk modulus B	1.5e3 [MPa]
reference friction velocity v_{ref}	1[mm/s]
Servovalve	
amplifier gain K_e	1 [A/V]
spool gain K_{spool}	0.0024 [m/A]
servovalve channel width b	5[mm]

Table 9.
Values of free (phenomenological) model parameters

Configuration parameters	Values
Hydraulic actuator	
piston friction force F_{fric_max}	50 [N]
product $Cd_{AB} A_{leak}$	3.2863e-3 [mm²]
Servovalve	
discharge coefficient Cd	0.2191 [-]
damping ratio ξ	0.3701 [-]
natural frequency $\omega_{n.servo}$	43 [Hz]

Table 8 specifies values of the physical and geometrical parameters used in the simulation model, while Table 9 specifies phenomenological ones to be estimated.

2.2. Estimation with use of Simulink® Parameter Estimation tool

The goal of this numerical study is to reconstruct (estimate) true values of the phenomenological parameters of the test-rig model, while the geometrical and physical parameters are known. The selected parameters and their true values are specified in Tables 10, 11 and 8, respectively to scenario A and B. The scenario A considers estimation of a single free parameter, while the scenario B considers estimation of two free parameters

simultaneously. The input to the model is the demanded displacement of the rod of the actuator, while the output is the measured (simulated) displacement. The boundary conditions were imposed on the estimating parameters values according to physical limitations. The iterative convergence process was run for a couple of minutes (15 min) to minimize the error objective function. The error was computed comparing reference system output (displacement) with predicted model output after each iteration. The estimated values of the parameters are presented in Tables 10, 11.

Table 10.
True and estimated values of the parameters - Case A

Parameter to be estimated	True value	Estimated value	error
flow coefficient [-]	5e-05	5e-05	0 %
natural frequency of the servovalve [Hz]	43	43	0 %
leakage flow from lower to upper chamber of actuator [m³/s],	1.5e-10	1.5e-10	0 %

Table 11.
True and estimated values of the parameters - Case B

Parameter to be estimated	True value	Estimated value	error
damping ratio of the servovalve	0.98	0.97297	0.7%
leakage flow from lower to upper chamber of actuator [m³/s],	1.5e-10	1.5031e-10	2%

The true values of the parameters were reconstructed without an error in the case A, while in the case B two free parameters were estimated with error lower than 2%. The case B shows difficulty in correct evaluation of the "true" value of the parameters when a few parameters is simultaneously estimated.

3. Summary

The paper proposes and demonstrates a first-principle data-driven approach towards modeling of technical systems [2-3]. The FPDD model offers physical insight and sufficient numerical performance to be applicable in understanding underlying physical phenomena, designing control systems, diagnosing and optimizing processes [4-13]. FPDD models can be used in many areas where physical understanding is critical, e.g. design of new products or early warning diagnostics of large industrial installations. The model is represented by nonlinear state-space equations having geometrical and physical parameters deduced from available documentation, and adjustable phenomenological

parameters (e.g. friction, leakage coefficients) that are estimated from measurement data.

The first part of the paper [14] provides a background discussing model taxonomy and parameter estimation methods, while this second part of the paper provides numerical examples of FPDD model performance focusing on estimation of single and multiple parameters.

Adjusting a FPDD model to data is, in most cases, a non-convex optimization problem and the criterion function may have several local minima [15]. It is therefore most natural to use physical insight to provide initial values to ensure robustness and fast convergence of the optimization process as well as to reduce the dimensionality of the parameters space by selecting only these parameters values of which are difficult to derive. Using physics-based initial conditions has significant advantage over blind (random) initialization of the optimization routine and furthermore, physical meaning of the parameters allows additional constraints to be set on the error function and/or model parameters narrowing the domain in which the optimum is being searched for. For example, the damping ratio in the model of the servo-valve system (Eq. 3) is limited in the range from zero to unity. Ranges of tunable model parameters constitute a hyper-cube in the so-called parameter space. The number of parameters defines dimensionality of such a space, for instance, if the model has two parameters, the parameter space is two-dimensional and ranges of the parameters form a rectangle. Optimization problem is stated by giving the parameter space, a criterion function and a domain over which the function is defined. Solving an optimization problem means finding extrema of the criterion function that are located within the domain. Typically, it suffices to find a single extremum located within proximity of a given point in the domain, to which end an iterative optimization process can be used. Constructing the criterion function requires multiple observed data points to be available and, ideally, to be uniformly distributed covering the entire operating range.

Future investigations are planned to focus on repeatability and reproducibility of the system identification results obtained for adjusting model parameters based on a number of operational data sets.

Acknowledgements

Nomenclature

t	continues time domain
$x(t)$	the n-dimensional state vector
$u(t)$	input
$y(t)$	output
K	bulk modulus of oil (oil stiffness) [N/m^2]
F	load [N]
x_{spool}	displacement of servo valve spool [m]
$x_{spool,min}$	lower position of servo valve spool [m]
$x_{spool,max}$	upper position of servo valve spool [m]
$x_{spool,0}$	dead zone of servo valve spool [m]
K_e	voltage-current amplifier proportional gain [A/V]
K_{spool}	current-displacement proportional gain [m/A]
K_P	PID proportional gain [V/m]
K_I	PID integral gain [V·s/m]
K_D	PID derivative gain [V/(m·s)]
T_I	PID integral time [s]
T_D	PID derivative time [s]
x_4	displacement of actuator [m]
$x_{4,expected}$	expected displacement of actuator [m]
Δx_4	difference between expected and obtained displacement of actuator [m]
u	spool voltage [V]
u_{PID}	output voltage from PID controller [V]
$\omega_{n,servo}$	Natural angular frequency of the servovalve [Hz]
ξ	Damping ratio of the servovalve [-]
p_A	pressure in the upper actuator chamber (chamber A) [Pa]
p_B	pressure in the lower actuator chamber (chamber B) [Pa]
p_P	pressure at the input of actuator (supply pump pressure) [Pa]
p_T	pressure at the output of actuator [Pa]
Δp_{PA}	pressure drop between input and lower chamber of actuator [Pa]
Δp_{PB}	pressure drop between input and upper chamber of actuator [Pa]
Δp_{AT}	pressure drop between lower chamber and output of actuator [Pa]
Δp_{BT}	pressure drop between upper chamber and output of actuator [Pa]
Δp_{AB}	pressure drop between lower and upper chamber of actuator [Pa]
q_A	sum of inflows and outflows to lower chamber of actuator [m^3/s]
q_B	sum of inflows and outflows to upper chamber of actuator [m^3/s]
q_{PA}	flow from input to lower chamber of actuator [m^3/s]
q_{PB}	flow from input to upper chamber of actuator [m^3/s]
q_{AT}	flow from lower chamber to output of actuator [m^3/s]
q_{BT}	flow from upper chamber to output of actuator [m^3/s]
q_{AB}	leakage flow from lower to upper chamber of actuator [m^3/s]
Cd	discharge coefficient [-]
b	width of servovalve flow hole [m]
A_A	area of cross-section of lower chamber of actuator [m^2]
A_B	area of cross-section of upper chamber of actuator [m^2]
$A_{leakage}$	area of leakage between upper and lower chamber of actuator [m^2]
V_A	volume of lower chamber of actuator [m^3]
V_B	volume of upper chamber of actuator [m^3]
V_{A0}	initial volume of lower chamber of actuator [m^3]
V_{B0}	initial volume of upper chamber of actuator [m^3]
m_4	mass of moving part of actuator (actuator piston, actuator rod, adapter) [m]

References

[1] Matlab/Simulink package documentation, The Math Works Inc., Natick 1998.

[2] K. Białas, Synthesis of mechanical systems including passive or active elements reducing of vibrations, Journal of Achievements in Materials and Manufacturing Engineering 20 (2007) 323-326.

[3] M. Annarumma, A. Naddeo, M. Pappalardo, Software independence: impact on automotive product development process Journal of Achievements in Materials and Manufacturing Engineering 31/2 (2008) 725-735.

[4] T. Dzitkowski, A. Dymarek, Design and examining sensitivity of machine driving systems with required frequency spectrum. Journal of Achievements in Materials and Manufacturing Engineering 26/1 (2008) 49-56.

[5] A. Naddeo, M. Annarumma, M. Pappalardo, N. Cappetti, State of the art of the passive pedestrian safety simulation, Journal of Achievements in Materials and Manufacturing Engineering 30/1 (2008) 51-58.

[6] S. Żółkiewski, Analysis and modelling of rotational systems with the Modyfit application, Journal of Achievements in Materials and Manufacturing Engineering 30/1 (2008) 59-66

[7] K. Białas, Comparison of passive and active reduction of vibrations of mechanical systems, Journal of Achievements in Materials and Manufacturing Engineering 18 (2006) 455-458.

[8] A. Buchacz, Influence of piezoelectric on characteristics of vibrating mechatronical system, Journal of Achievements in Materials and Manufacturing Engineering 17 (2006) 229-232.

[9] A. Buchacz, S. Żółkiewski, Dynamic analysis of the mechanical systems vibrating transversally in transportation, Journal of Achievements in Materials and Manufacturing Engineering 20 (2007) 331-334.

[10] J. Świder, G. Wszołek, K. Foit, P. Michalski, S. Jendrysik, Example of the analysis of mechanical system vibrations in GRAFSIM and CATGEN software, Journal of Achievements in Materials and Manufacturing Engineering 20 (2007) 391-394.

[11] J. Świder, A. Baier, Aided design, virtual development and testing of modern control systems, Proceedings of the 11th International Scientific Conference "Achievements in Mechanical and Materials Engineering" AMME'2002, Gliwice-Zakopane, 2002, 541-544 (in Polish).

[12] J. Świder, G. Kost, J. Gorczyński, Process control technology using logic controllers PLC, Proceedings of the 11th International Scientific Conference "Achievements in Mechanical and Materials Engineering" AMME'2002, Gliwice-Zakopane, 2002, 549-552 (in Polish).

[13] J. Świder., R. Zdanowicz, Application of PLC controller in the systems simulation model Proceedings of the 12th International Scientific Conference "Achievements in Mechanical and Materials Engineering" AMME'2003, Gliwice-Zakopane, 2003, 971-974 (in Polish).

[14] P. Czop, G. Kost, D. Sławik, G. Wszolek, Demonstration of First-Principle and Data-Driven Models Using Numerical Case Studies: Part A. Journal of Achievements in Materials and Manufacturing Engineering 44/2 (2010)

[15] T. Bohlin, Practical Grey-box Process Identification: Theory and Applications (Advances in Industrial Control), Springer-Verlag, London, 2006.